Stress–strain curves of superplastic alloys

A. JUHÁSZ, P. TASNÁDI, N. Q. CHINH, I. KOVÁCS
Institute for General Physics, Eötvös University, Budapest, Hungary

Force–elongation and stress–strain curves have been analysed for superplastically deformed alloys tested in uniaxial tension under constant cross-head velocity conditions. By considering instability criteria the curves can be divided into three characteristic stages. In the course of the first two stages the samples are work hardened while during the third stage no work hardening takes place, although 85 to 90% of the total deformation occurs at this stage. However, sometimes at the end of stage III a weak strain hardening appears again due to grain growth. From the analysis of stage III the strain-rate sensitivity can be determined in good agreement with other methods.

1. Introduction

Superplasticity is a well-known phenomenon investigated most often by tensile testing. The experimental and theoretical aspects of superplastic flow are well documented and there are excellent reviews of the subject [1–3]. Superplastic metals are generally capable of high tensile elongation so that failure occurs after a few hundred (or thousands) per cent tensile strain. The tensile strain, ε, of a material can be given by the expression

$$\varepsilon = \int_0^t \dot{\varepsilon}\,(\sigma, T, \alpha_1, \alpha_2, \ldots)\,\mathrm{d}t \qquad (1)$$

where t is the time interval investigated and $\dot{\varepsilon}$ is the strain rate which depends on the stress, the temperature and some structural parameters $\alpha_1, \alpha_2, \ldots \alpha_i$. These structural parameters may be, for example, the grain size, the grain aspect ratio, the grain-size distribution, etc. The general form of the $\dot{\varepsilon}(\sigma, T, \alpha)$ function is not known, but in the case of superplastic materials a generally accepted assumption is that in a wide range of the conditions of deformation the structure of the material is stable, so macroscopic necking and microscopic changes do not take place. Theories of tensile deformation predict a correlation between the magnitude of strain-rate sensitivity, m, and the total elongation of the samples [4, 5]. However, more rigorous examinations show that even if the deformation can be regarded as superplastic, structural changes occur and a suitable magnitude of strain-rate sensitivity is only a necessary but not a sufficient parameter in predicting the optimum superplastic ductility.

According to Langdon [6] the local strain may vary along the gauge length even in the superplastic region. For example, the deformation of a Zn–22Al alloy was uniform up to about 150% and thereafter were slight perturbations on the local strain along the gauge length. This test proved that in the superplastic region the deformation was quasistable with diffuse neck formation [6].

Another experimental result is that in some cases strain hardening occurs up to some strain level [7]. During this early part of the deformation the flow stress is significantly dependent on strain. The strain at which saturation in flow stress is attained depends on the strain rate and temperature. The strain hardening may occur, for example, as a consequence of grain coarsening.

Because the evolution of the stable microstructure, which is necessary for quasistable superplastic flow, is strongly dependent on the details of the deformation, the rigorous consideration of these details is very important in the evaluation of the results of the measurements. To characterize the deformation, true stress–true strain or engineering stress–engineering strain curves are generally used. In a recent paper, Baudelet and Suery [8] have given a detailed analysis of various types of tensile deformation modes. They also discuss the conditions of superplasticity at constant strain rate and at constant true stress. However, the tensile deformation of superplastic materials is usually performed at constant cross-head velocity. In this paper we deal with this deformation mode in the case of Al–Zn–Mg, Al–Zn–Mg–Fe–Zr and, as a reference material, of eutectic Pb–Sn alloys. The analysis of the deformation will be based on the force–elongation and true stress–true strain curves. In a previous paper it was demonstrated that Al–Zn–Mg alloys close in composition to that produced commercially can be made to exhibit superplasticity by the addition of zirconium as a grain-refining element [9].

Assuming that the volume of the samples is constant and introducing stability criteria other than the classical one, it is shown in this paper that the stress–strain curves of the superplastic materials can be described in a unique way.

2. Experimental details

Superplastic Al–Zn–Mg alloys and eutectic Pb–Sn alloy were investigated by tensile testing at constant cross-head velocity in an air furnace attached to an Instron machine. The tensile specimens were spark machined from sheets 2 mm thick with a gauge length of 6.5 mm (Fig. 1). The chemical composition of the alloys investigated and the experimental conditions are given in Table I.

0022–2461/87 $03.00 + .12

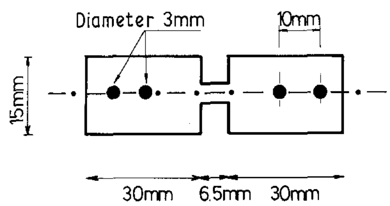

Figure 1 The tensile specimen.

Fig. 2 shows the force–elongation curves of an AlMgZnZrFe alloy deformed at different cross-head velocities at 500° C. True stresses and strains were determined with the assumptions that the volume of the sample is constant and the elongation is uniform in the course of the test. The true stress–true strain curves belonging to the force–elongation curves in Fig. 2 are shown in Fig. 3. These results show that although the samples were generally elongated to a great extent, really superplastic deformation took place only in the case of 0.2 and 0.5 mm min^{-1} cross-head velocities at which the total elongation reaches 450%.

In the following section the typical superplastic stress–strain curves will be analysed. Such curves are shown in Fig. 4 for AlMgZnZr, AlMgZnZrFe and for eutectic Pb–Sn alloys.

3. Results and discussion

3.1. Stages of superplastic deformation

According to the experimental results, the force–elongation and stress–strain curves of the samples deformed superplastically can be characterized schematically by the curves shown in Figs 5 and 6.

These curves can be divided into three stages separated by different stability criteria. Let us denote the onset of the three stages of the force elongation curves by l_0, l_1 and l_2. The same positions on the stress–strain curves are denoted by $\varepsilon = 0$, ε_1 and ε_2, respectively. In the region of

$$l_0 \leqslant l \leqslant l_1 \quad (2)$$

or

$$0 \leqslant \varepsilon \leqslant \varepsilon_1 \quad (3)$$

the force is increasing monotonically, the deformation is stable and the elongation is uniform. The upper limit (l_1, ε_1) of stage I can be determined by the well-known stability criterion of Considère:

$$\frac{dP}{dl} \geqslant 0 \quad (4)$$

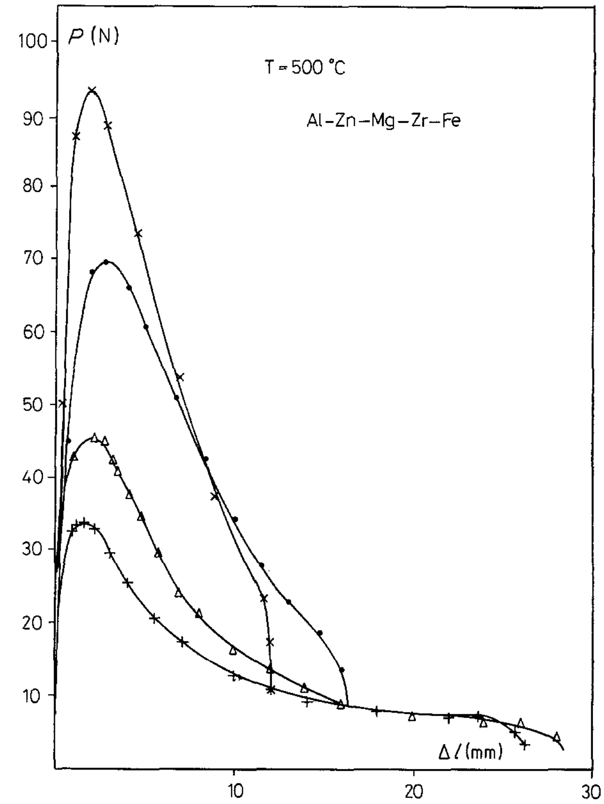

Figure 2 Force–elongation curves of AlMgZnZrFe samples deformed at different cross-head velocities. $T = 500°$C, (×) sample 8, (●) sample 7, (△) sample 6, (+) sample 4.

where P is the applied force. In the region of uniform strain the true stress is given by

$$\sigma = \frac{P}{q} \quad (5)$$

where q is the cross-section of the sample. Considering that the volume of the sample is constant, that is

$$d(ql) = 0 \quad (6)$$

therefore

$$\frac{dq}{q} = -\frac{dl}{l} = -d\varepsilon \quad (7)$$

By using this formula, the Considère criterion can be written in the form:

$$\frac{dP}{dl} = q\frac{d\sigma}{dl} + \sigma\frac{dq}{dl} = q\frac{d\sigma}{dl} - \frac{q}{l}\sigma = \frac{q}{l}\left(\frac{d\sigma}{d\varepsilon} - \sigma\right) \geqslant 0 \quad (8)$$

TABLE I

Number of samples	Chemical composition	Experimental conditions	
		Cross-head velocity (mm min^{-1})	Temperature (° C)
1	Pb–Sn eutectic	0.5	148
2	Al–4.8Zn–1Mg–0.5Zr	0.5	500
3	Al–4.8Zn–1Mg–0.5Zr–0.15Fe	0.2	454
4	as above	0.2	500
5	as above	0.2	525
6	as above	0.5	500
7	as above	2.0	500
8	as above	3.0	500

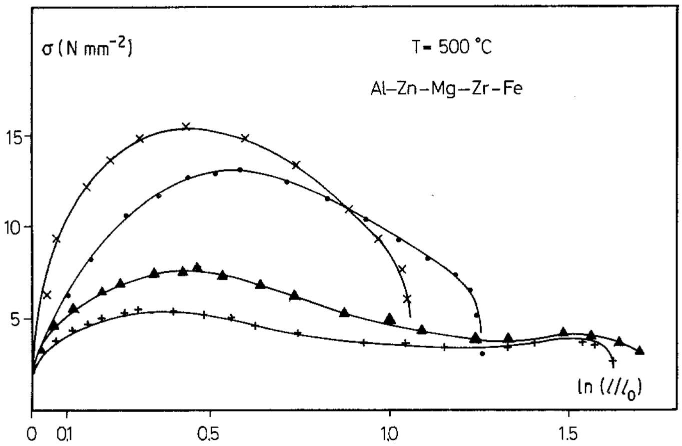

Figure 3 True stress–true strain curves of AlMgZnZrFe samples. T = 500° C, (×) sample 8, (●) sample 7, (▲) sample 6, (+) sample 4.

From this we obtain

$$\frac{d\sigma}{d\varepsilon} \geqslant \sigma \tag{9}$$

i.e. the limit of stage I can be determined from the equation

$$\left(\frac{d\sigma}{d\varepsilon}\right)_{\varepsilon=\varepsilon_1} = \sigma(\varepsilon_1) = \sigma_1 \tag{10}$$

According to this, a tangent can be drawn to the true stress–true strain curve at the point (σ_1, ε_1) with the method shown in Fig. 6. If this construction fits the curves measured then it proves that the deformation is uniform and stable.

By the use of the expression, $\varepsilon = \ln(l/l_0)$ and equations 5 and 6, the true stress can be written in the form

$$\sigma = \frac{P}{q_0} e^{\varepsilon}, \tag{12}$$

where q_0 is the initial cross-section. From this it can be seen that the true stress increases monotonically in the neighbourhood of ε_1.

For strains $\varepsilon > \varepsilon_1$ the stability criterion (Equation 9) is not satisfied. In the case of normal (not superplastic) material this means that necking takes place and the sample fractures quickly. In the case of superplastic deformation, ε_1 is much less than the maximum strain and macroscopic necks do not develop for strains $\varepsilon > \varepsilon_1$. This means that the deformation still can be regarded as uniform in stage II. In this region $\varepsilon_1 < \varepsilon < \varepsilon_2$, and the equation

$$\frac{d\sigma}{d\varepsilon} \geqslant 0 \tag{13}$$

is used as a stability criterion.

To point out the existence of stage II on the force–elongation diagram one must express $d\sigma/d\varepsilon$ with dP/dl

$$\frac{d\sigma}{d\varepsilon} = \frac{d}{d\varepsilon}\left(\frac{P}{q_0} e^{\varepsilon}\right) = \frac{1}{q_0}\left(e^{\varepsilon}\frac{dP}{d\varepsilon} + Pe^{\varepsilon}\right) \tag{14}$$

Considering $d\varepsilon/dl = 1/l$, Equation 14 can be written in the form

$$\frac{d\sigma}{d\varepsilon} = \frac{e^{\varepsilon}}{q_0}\left(l\frac{dP}{dl} + P\right) \tag{15}$$

By using this equation the stability criterion (Equation 13) can be given by the relationship

$$\frac{dP}{dl} \geqslant -\frac{P}{l} \tag{16}$$

The end of the validity of this relationship can be obtained graphically by drawing a tangent to the force–elongation curve at such a point (l_2, P_2) where the tangent is parallel to the segment (O, P_2) (l_2, O). As it can be seen from Equation 15 the equivalent point on the stress–strain curve belongs just to its maximum.

Stage III begins at $\varepsilon = \varepsilon_2$. According to the experiments, the majority of the deformation takes place in this stage, so the flow should be stable in this region too. For this stage we consider the equation

$$\left(\frac{d\sigma}{d\varepsilon}\right)_{\dot{\varepsilon}} = 0 \tag{17}$$

as a stability criterion. This means that the flow stress is independent from the strain in this stage and it depends only on the strain rate and the structural parameters of the sample. According to Fig. 6 stage

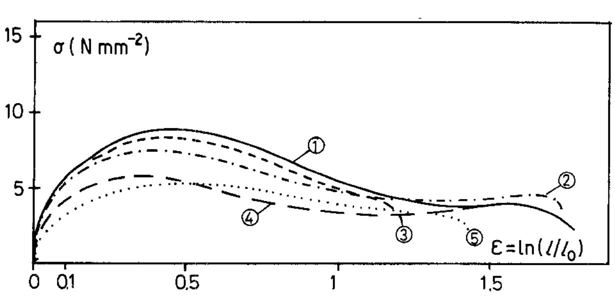

Figure 4 Stress–strain curves of samples 1 to 5.

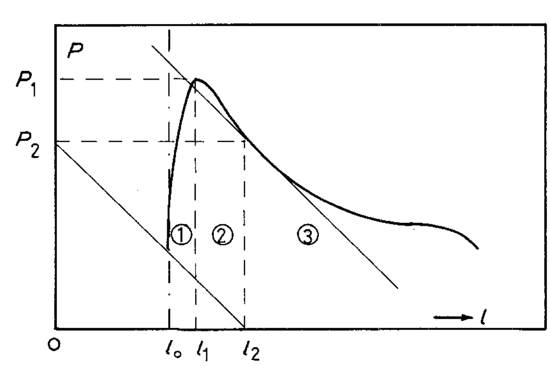

Figure 5 Schematic force–elongation curve illustrating the stages of superplastic deformation.

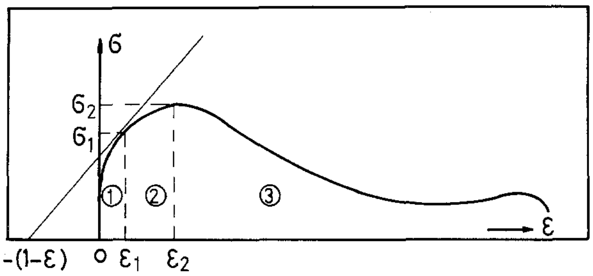

Figure 6 Schematic stress–strain curve illustrating the stages of superplastic deformation.

III is a large region after the maximum of the $\sigma = \sigma(\varepsilon)$ function.

The decrease of σ with increasing ε contradicts seemingly the stability criterion (Equation 17). However, taking into account the fact that in the course of the deformation the strain rate is decreasing monotonically, the paradox can be resolved.

Assuming that in stage III there is no strain hardening, the connection between the stress and the strain rate can be given by the equation

$$\sigma = C\dot{\varepsilon}^m \tag{18}$$

where C is a proportionality factor depending on the temperature and the structural parameters of the sample. In a first approximation the strain-rate sensitivity, m, can be regarded as constant, because the order of magnitude of $\dot{\varepsilon}$ does not change in stage III. By using Relation 18 the ratio of any two stresses, σ_i and σ_j is

$$\frac{\sigma_i}{\sigma_j} = \left(\frac{\dot{\varepsilon}_i}{\dot{\varepsilon}_j}\right)^m \tag{19}$$

In the case of constant cross-head velocity the strain rate is

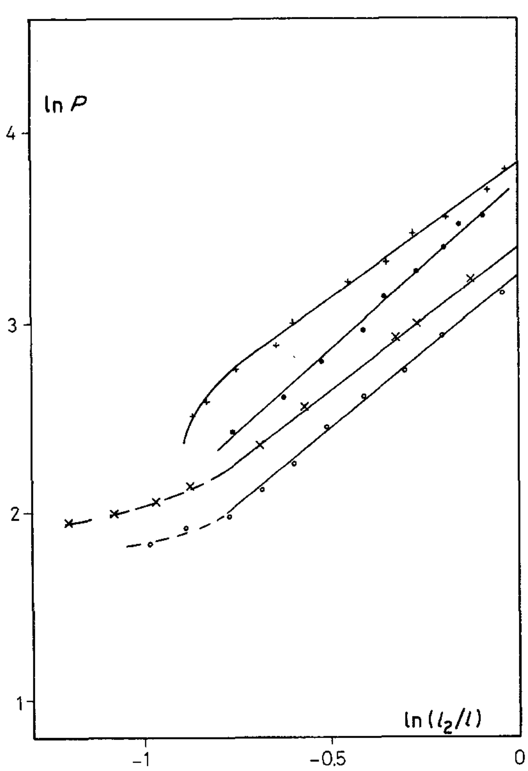

Figure 7 The ln$P$-ln (l_2/l) relationship in stage III of superplastic deformation. (●) Sample 1, (×) sample 4, (+) sample 3, (O) sample 5.

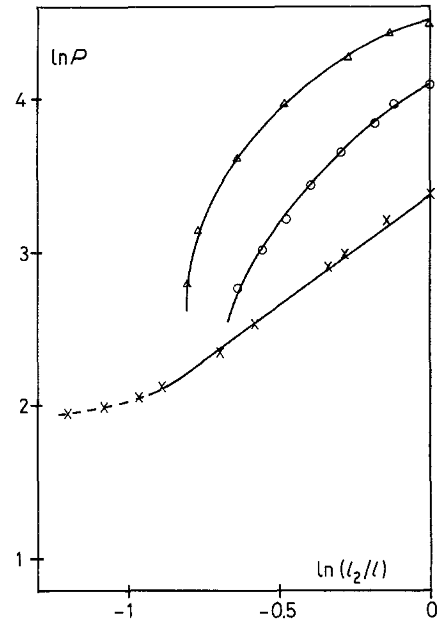

Figure 8 The ln$P$-ln (l_2/l) relationship for the AlZnMgZrFe alloy at different cross-head velocities. (×) Sample 4, (O) sample 7, (△) sample 8.

$$\dot{\varepsilon} = \frac{v}{l} \tag{20}$$

With the constancy of the volume Relationship 19 can be expressed with the force and elongation in the form

$$\frac{P_i}{P_j} = \left(\frac{l_j}{l_i}\right)^{m+1} \tag{21}$$

Using P_2, l_2 as P_j, l_j and dropping the index i we can write:

$$P = P_2\left(\frac{l_2}{l}\right)^{m+1} \tag{22}$$

or by taking the logarithm of this equation:

$$\ln P = \ln P_2 + (m + 1)\ln\frac{l_2}{l} \tag{23}$$

Plotting ln$P$ as a function of ln (l_2/l) a straight line should be obtained in stage III. Fig. 7 shows that Equation 23 is valid at every temperature for all the alloys investigated. The strain-rate sensitivities obtained from the slopes of the ln$P$-ln (l_2/l) curves agree well with that determined by the strain-rate change method at the strain $\varepsilon \approx 0.5$. The relatively high values of the obtained strain-rate sensitivities, $m \geqslant 0.45$, together with some other results published in a previous paper [9] prove that the deformation of the samples investigated is superplastic. In the case of higher cross-head velocities Equation 23 could not be fitted to the force–elongation curves. According to Fig. 8, for Al–Zn–Mg–Zr–Fe samples tested at 500° C with different cross-head velocities, Equation 23 fits well to the experimental data only in the case of $v = 0.2\,\mathrm{mm\,min^{-1}}$. Fig. 9 shows the true stress–true strain curve of a sample deformed superplastically at 500° C with $0.2\,\mathrm{mm\,min^{-1}}$ cross-head velocity. The continuous line represents Equation 19. Initially, the experimental points lie along this curve, but at the end of the deformation the measured σ values are significantly greater than the values calculated. This

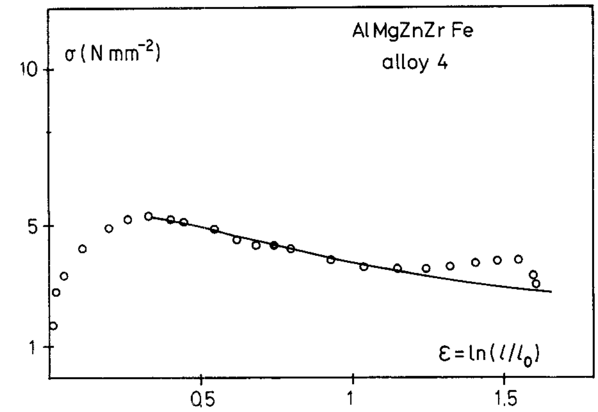

Figure 9 Theoretical (——) (Equation 19) and experimental (○) stress–strain curve in stage III of sample 4.

deviation is probably due to the decrease of the strain-rate sensitivity with the increasing deformation. In this last period of the deformation the true stress again increases slightly, that is

$$\frac{d\sigma}{d\varepsilon} > 0 \qquad (24)$$

It is worth determining this condition by the use of Equation 18. Taking its logarithm after differentiation by $\dot{\varepsilon}$ we obtain

$$\frac{1}{\sigma}\frac{d\sigma}{d\dot{\varepsilon}} = \ln\dot{\varepsilon}\frac{dm}{d\dot{\varepsilon}} + \frac{m}{\dot{\varepsilon}} \qquad (25)$$

By using Equation 20 we obtain $d\dot{\varepsilon} = -\dot{\varepsilon}d\varepsilon$, therefore Equation 25 can be written in the form

$$\frac{1}{\sigma}\frac{d\sigma}{d\varepsilon} = -\ln\dot{\varepsilon}\frac{dm}{d\ln\dot{\varepsilon}} - m \qquad (26)$$

According to this, Equation 24 can be satisfied if

$$-m - \ln\dot{\varepsilon}\frac{dm}{d\ln\dot{\varepsilon}} > 0 \qquad (27)$$

As $\ln\dot{\varepsilon} < 0$, this condition can be fulfilled only if $dm/d\ln\dot{\varepsilon}$ is positive. This means that at the end of the deformation the strain rate becomes so small that the corresponding m value decreases with decreasing strain rate. Characterizing the deformation on the basis of the well-known maximum curve of $m - \ln\dot{\varepsilon}$, it can be seen that the deformation discussed above takes place at very low strain rates which are due to the first increasing part of this curve [9]. Similar results were obtained by Müller and Rassmann [10] for a ternary eutectic PbSnCd alloy.

This hardening effect can be explained by grain coarsening. A series of pictures in Fig. 10 shows that during the superplastic deformation, continuous grain coarsening takes place.

4. Conclusions

The superplastic tensile deformation process at constant cross-head velocities of some AlZnMg and the eutectic Ps–Sn alloys can be divided into three stages characterized by different stability criterions. The first stage terminates at the maximum force. In the course of stage II the force decreases monotonically but the flow stress increases. Stage II terminates at the maximum stress.

The strain rate decreases continuously during deformation. In the first two stages there is a significant work hardening. After reaching the peak stress at about $\varepsilon = 50\%$, in stage III a deformation structure develops in the samples which remains stable up to about strains of 250 to 300%. In this stage the flow stress depends only on the strain rate. Because it is decreasing continuously, the flow stress decreases monotonically as well. The strain-rate sensitivity determined from the data of stage III is in good agreement with the results obtained by other methods.

At the end of stage III work hardening may appear again as a consequence of grain coarsening.

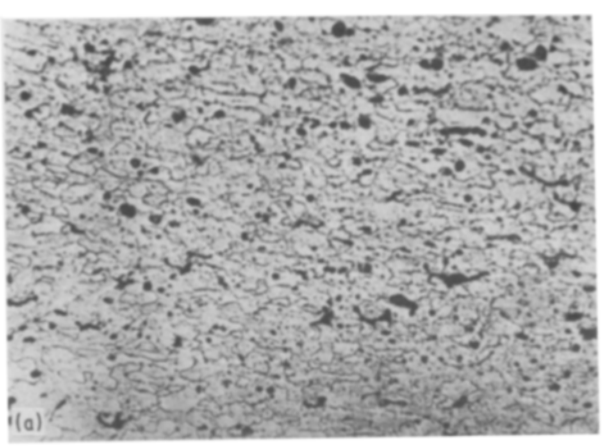

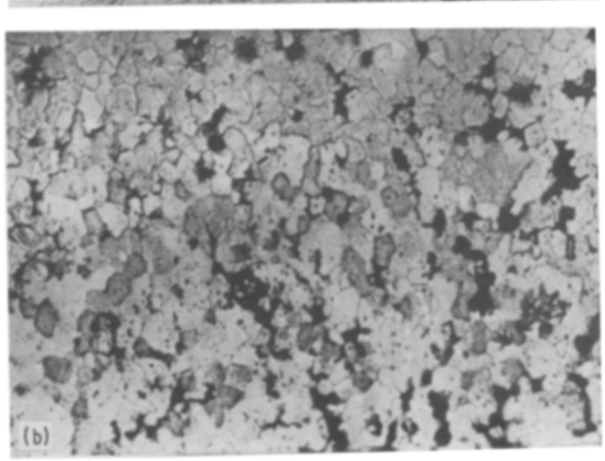

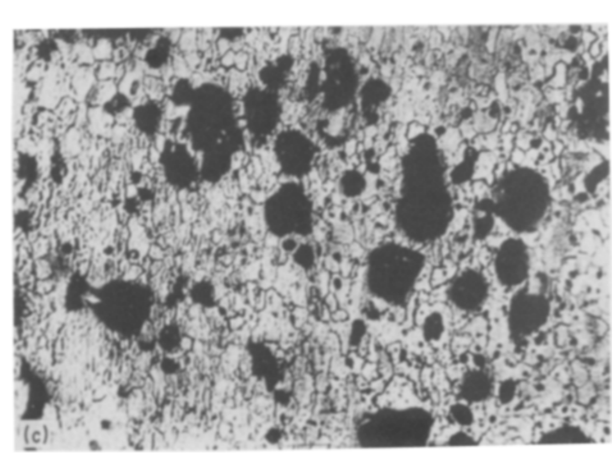

Figure 10 Change of grain structure during superplastic deformation of sample 2. The pictures were taken at strains $\varepsilon = 0.7$ (a) $\varepsilon = 1.12$ (b) and $\varepsilon = 1.67$ (c).

References

1. R. H. JOHNSON, *Metal. Rev.* **15** (1970) 115.
2. J. H. GITTUS, "Mechanics of Solids", edited by H. G. Hopkins and M. J. Sewell (Pergamon, London, 1982) p. 227.
3. T. G. LANGDON, *Metall. Trans.* **13A** (1982) 682.
4. F. A. MOHAMED, M. M. I. AHMED and T. G. LANGDON, *ibid.* **8A** (1977) 933.
5. M. M. I. AHMED and T. G. LANGDON, *ibid.* **8A** (1977) 1832.
6. T. G. LANGDON, *Metall. Sci.* **16** (1982) 175.
7. B. P. KASHYAP and A. K. MUKHERJEE, "Strength of Metals and Alloys", edited by R. C. Gifkins (Pergamon, London, 1982) p. 707.
8. B. BAUDELET and M. SUERY, International Conference on Superplasticity, Grenoble, 16-19 September 1985 (Editions du C. N. R. S., Paris, 1985) p. 17.1.
9. A. JUHÁSZ, N. Q. CHINH, P. TASNÁDI, I. KOVÁCS and T. TURMEZEY, *J. Mater. Sci.* **22** (1987) 137.
10. P. MÜLLER and P. RASSMANN, *Z. Metallkde* **66** (1975) 213.

Received 17 October 1986
and accepted 29 January 1987